Geological Survey of Canada

CURRENT RESEARCH
2001-E12

Remote sensing as a geological mapping tool in the Arctic: preliminary results from Baffin Island, Nunavut

J.R. Harris, B. Eddy, A. Rencz, E. de Kemp, P. Budkewitsch and M. Peshko

Natural Resources Canada
Ressources naturelles Canada

Canada

Catalogue No. M44-2001/E12E-IN
ISBN 0-662-30775-5

Available in Canada from the
Geological Survey of Canada Bookstore website at:
http://www.nrcan.gc.ca/gsc/bookstore (Toll-free: 1-888-252-4301)

A copy of this publication is also available for reference by depository libraries across Canada through access to the Depository Services Program's website at http://dsp-psd.pwgsc.gc.ca

Price subject to change without notice

Remote sensing as a geological mapping tool in the Arctic: preliminary results from Baffin Island, Nunavut

J.R. Harris, B. Eddy[1], A. Rencz, E. de Kemp, P. Budkewitsch[2] and M. Peshko[3]
Continental Geoscience Division, Ottawa

Harris, J.R., Eddy, B., Rencz, A., de Kemp, E., Budkewitsch, P., and Peshko, M., 2001: Remote sensing as a geological mapping tool in the Arctic: preliminary results from Baffin Island, Nunavut; Geological Survey of Canada, Current Research 2001-E12, 13 p.

[1] GSI – GeoSystems Integration, 56 Fourth Avenue, Suite 1, Ottawa, Ontario K1S 2L2

[2] Canada Centre for Remote Sensing, 588 Booth Street, Ottawa, Ontario K1A 0Y7

[3] Noranda Exploration Ltd., 181 Bay Street, Suite 4100, P.O. Box 755, BCE Place, Toronto, Ontario M5J 2T3

Abstract

A study involving the application of remote sensing technology for geological mapping in arctic environments has been initiated in southern Baffin Island. Various remotely sensed imagery, characterized by different wavelengths and spatial and spectral resolutions, have been or is presently being acquired.

This area has been chosen as it represents a typical arctic geological and biophysical environment. It has a variety of lithologies ranging from gneissic and/or granitoid basement rocks to rift-related volcanic and sedimentary rocks to younger overlying Paleozoic sediments, and has been mapped on a regional scale (1:100 000) by the Geological Survey of Canada.

Particularly relevant for this project is the recent advancement of hyperspectral remote-sensing technology. Eleven lines of high-resolution hyperspectral data have been acquired using the Noranda Probe sensor over the study area. Preliminary results indicate that the optical sensors (Landsat TM and Probe) provide useful information with respect to compositional layering, structural patterns, and vegetation.

Résumé

Une étude faisant appel aux techniques de télédétection appliquées à la cartographie géologique en milieu arctique a été entreprise dans le sud de l'île de Baffin. Diverses images de télédétection ayant recours à des longueurs d'onde ou à des résolutions spatiales et spectrales différentes ont été enregistrées ou sont en voie de l'être.

Cette région a été retenue car elle représente des conditions géologiques et biophysiques typiques du milieu arctique. On y trouve une variété de lithologies allant des roches gneissiques ou granitoïdes de socle à des roches sédimentaires de couverture plus récentes du Paléozoïque, en passant par des roches volcaniques et sédimentaires associées à des processus de rifting. En outre, elle a été cartographiée à l'échelle régionale (1/100 000) par la Commission géologique du Canada.

Les innovations technologiques en télédétection hyperspectrale sont particulièrement pertinentes pour ce projet. Onze lignes de données de télédétection hyperspectrale haute résolution ont été acquises dans cette région d'étude à l'aide du capteur hyperspectral Probe de la Noranda. Les résultats préliminaires révèlent que les capteurs optiques (LANDSAT TM et Probe) fournissent des données utiles sur le rubanement de composition, les motifs structuraux et la végétation.

INTRODUCTION

A study of the application of remote-sensing technology for geological mapping in arctic terrain has been initiated as part of the central Baffin Island mapping project (St-Onge et al., 2001; Corrigan et al., 2001) supported and funded by the GSC Proposal Acceptance System (PAS). A test site in southern Baffin Island, approximately 80 km south of Iqaluit has been chosen (**Fig. 1**). Various types of remotely sensed imagery, characterized by different spatial and spectral resolutions, are being collected over the test site to evaluate the usefulness of remotely sensed imagery for assisting geological mapping in remote arctic environments.

Good bedrock exposure and the lack of continuous vegetation cover in the Arctic Archipelago provide an ideal environment for the application of remote sensing, using both optical-infrared and radar sensors, to characterize lithology, structure, and alteration patterns. Excessive vegetation cover in southern Canada has mitigated against the successful use of remote sensing for lithological and alteration mapping in previous studies. Although widely used in similar vegetation-poor areas of Australia and the United States (Sabins, 1992), satellite-derived spectral and radar imagery have not been systematically tested for the purpose of mapping and mineral exploration in the Canadian Arctic.

Southern Baffin Island (Fig. 1) has been selected for testing satellite, airborne, and ground spectral data for characterizing different lithological units and alteration targets. This area has been chosen as it represents a typical arctic environment. It has a variety of lithologies ranging from gneissic and/or granitoid basement rocks to rift-related volcanic and sedimentary rocks to younger overlying Paleozoic sediments, and has been mapped on a regional scale (1:100 000) by the Geological Survey of Canada (St-Onge et al., 2001).

Specifically, this project will 1) develop new methodologies in support of the production of geological and mineral exploration maps using a variety of remotely sensed data and, 2) apply existing methodologies (classification using maximum likelihood and neural networks) for producing geological and mineral exploration maps. The data includes current satellite data sources (e.g. Landsat, Radarsat) as well as new sensors such as the Probe hyperspectral system flown by Noranda Exploration Ltd., and the new NASA Aster sensor. A ground component will be undertaken to sample the various rock types for spectral, chemical, and mineralogical characteristics. This ground information will be fundamental to a proper interpretation of the remotely sensed data. The assessment will require computer analysis of remotely sensed data verified through field-based studies.

Particularly relevant for this project is the recent advancement of hyperspectral remote-sensing technology. Instead of a limited number of bands over a given portion of the electromagnetic spectrum, hyperspectral data comprise many bands of very narrow bandwidth. This typically means less than a two hundred nanometre bandwidth and, depending on the sensor, from 64 to 256 different bands. Studies of mineral spectroscopy make use of the visible through short-wave infrared portions of the electromagnetic spectrum (Clark, 1999). Spectra in this range are known to provide information on characterizing minerals and rock types. Subtle differences in absorption features can be attributed to mineralogy, chemical composition, grain size, and other factors. This information can then be applied to a variety of applications, including but not exclusively, alteration detection, mine-tailing characterization, and bedrock and surficial geology mapping.

The remotely sensed data used in this study represents a wide range of spectral measurements from various portions of the electromagnetic spectrum, sampled at different spatial and spectral resolutions. One of the principal aspects of this study, in terms of developing new methodologies for geological mapping in the arctic, is to compare the advantages of each data type, how new information may be derived from combining two or more data types through data fusion techniques, and to determine levels of quality control required on the use of remotely sensed data with ground spectroscopy and geochemistry data.

This paper presents preliminary results from visual inspection of enhanced Landsat TM, Radarsat, and hyperspectral remotely sensed data acquired over the test site. These results have not been verified by follow-up fieldwork, although a field campaign is planned for the summers of 2001 and 2002 to verify observations and maps produced from analysis of the remotely sensed data.

STUDY AREA

The McKellar Bay area (**Fig. 2**) is comprised of three Paleoproterozoic tectonostratigraphic assemblages that were accreted to the Archean Superior Province during the Trans-Hudson Orogen (St-Onge et al., 2001). The study area defined by the coverage of the hyperspectral and remote sensing data is underlain by the Narsajuaq Arc, and Lake Harbour Group, which are intruded by the Cumberland Batholith. Polyphase deformation and metamorphism affected the Narsajuaq Arc and Lake Harbour Group rocks, resulting in complex north-south, northwest-southeast sinusoidal, interference fold patterns (mushroom-style folds). All rocks exhibit compositional layering.

The subareas (field study areas) shown in Figure 2 were selected from an initial examination and interpretation of the raw hyperspectral and Landsat TM data. **Table 1** summarizes some of the features that will be studied in the hyperspectral and remote sensing data. These features (compositional layering, structure, etc.) can be mapped systematically throughout the study area at an approximate 5–30 m resolution using the remotely sensed data. This resolution is comparable to mapping at a 1:5000 to 1:50 000 scale, and therefore is expected to reveal considerable detail in the distribution of rock types, structure, and associative mineralogy.

METHOD AND DATA DESCRIPTION

The remote sensing data include current satellite data sources (e.g. Landsat, Radarsat) as well as airborne hyperspectral data, and conventional orthophotos (**Table 2**). The hyperspectral data were collected during the summer of 2000 using the Probe system flown by Noranda Exploration Ltd. Data will also be collected from the new NASA Aster satellite during the summer 2001. A field study component will be undertaken during the summer 2001 to sample the various rock types for spectral, chemical, and mineralogical characteristics. This information will be fundamental to a proper interpretation of the remotely sensed data.

The Landsat TM data (both 5 and 7) have been used successfully for geological and alteration mapping in numerous studies (Harris et al., 1998), including the north Baffin Island study (Rencz et al., 2000). Landsat is also particularly useful for generating a vegetation mask that can be used to subset the hyperspectral data, and other data to reveal the exposed bedrock areas (*see* Harris et al., 1998). Spectral properties of the vegetated and nonvegetated areas will be compared using this procedure.

The Radarsat data provides information on structure, texture, and surface morphology. This can be incorporated directly into the quantitative analysis of the Landsat TM and hyperspectral data by adding a radar texture image as a theme in an IHS fusion (Harris et al., 1990). This data fusion method is useful as an aid in interpretation, and/or as a mask for discriminating rock types on the basis of surface texture.

The Aster data is a new sensor available from the NASA's EOS satellite. This data provides 15 bands covering the visible-near infrared (VNIR), shortwave infrared (SWIR), and thermal infrared (TIR) portions of the EM spectrum. Analysis of the Aster VNIR and SWIR channels will be compared with results from the Landsat TM and hyperspectral data, and the thermal bands will be used to examine the thermal spectral properties of the rock types and mineralogy in the study area.

Whereas the bands in the Landsat, Radarsat, and Aster data record information along 'wide' intervals of the EM spectrum (i.e. broad band intervals), the hyperspectral data records a continuous spectrometric profile from the VNIR to SWIR range (0.4–2.5 μm) for each 5 m pixel in the study area. Eleven lines of hyperspectral data that cover a 60 km x 30 km area (**Fig. 2**) provide over 50 000 000 spectral 'profile' samples for the study area. The spectral signature for each pixel, derived from 128 data channels, is influenced by the spectroscopic properties of the materials that reside in each pixel, including exposed bedrock, overburden, and vegetation. The processing of these data will involve spectral 'unmixing' to discriminate rock types and mineralogy present in exposed bedrock areas. Ground spectrometry data for each test area (Fig. 2) will be collected to provide ground truth and calibration for the processing, analysis, and interpretation of the hyperspectral data.

It is expected that the hyperspectral data, when used in combination with the Landsat TM, Radarsat, and ground spectrometry and geochemistry, will yield new information on the structural and chemical compositional variation in the rocks. Successful application of these data is expected to reveal more detailed information on the location, geometry, and spatial distribution of the many lithologies, and possibly their associative mineral assemblages. From these spatially referenced lithological distribution patterns, it may be possible to reveal patterns of metamorphic grade in relation to deformation fabrics, compute lithological volume estimates, and/or examine the geochronological relationships in greater detail.

PRELIMINARY RESULTS

Visual analysis of the remotely sensed data was conducted during the winter and spring 2001 in preparation and selection of field study areas for summer fieldwork. **Figures 3, 4**, and **5** show several views of the different data sets for two test sites (locations shown *in* Fig. 2). Each area is comprised of all three tectonostratigraphic assemblages discussed above, in locations where the polyphase deformation and compositional layering is most prominent. This preliminary comparative analysis illustrates the effects of the differences in the spatial and spectral resolutions in the different data sets, and helps reveal the significant contrast in the level of detail in the hyperspectral data (Fig. 5). A geological map of each site derived from St-Onge et al. (2001) is provided for comparison to the remotely sensed data.

Previous results obtained from applying image analysis classification techniques to Landsat 5 and airborne magnetic data for discriminating lithology in this area (Schetselaar and de Kemp, 2000) revealed that Landsat could discriminate between basement and cover rocks with an accuracy of approximately 71% using the mapped geology (St-Onge et al., 2001) as a base for comparison. The magnetic data resulted in an accuracy of approximately 74% and when both data types were combined, an accuracy of close to 77% was achieved.

Figure 3 shows several views of the remotely sensed data centred over a series of northwest-southeast-plunging fold structures defined by the Lake Harbour Group, within the Narsajuac Arc granitic rocks (*see* **Fig. 2** for location). Figure 3a shows a Landsat TM 5, colour composite image, Figure 3b is a radar (Radarsat – S6 mode) image, and Figure 3c is the mapped geology (St-Onge et al., 2001) for test site 1. Figure 3d shows an airborne shadow-enhanced magnetics image. The Landsat image comprises three bands: 1) 0.45–0.52 μm (micrometres) — visible energy displayed in blue, 2) 1.55–1.75 μm — near infrared energy displayed in red, and 3) 2.08–2.35 μm — shortwave infrared energy displayed in green. Both the Landsat and Radarsat images have been contrast enhanced.

Various hues can be seen on the Landsat image, some of which correlate with the mapped geology. The bluish purple hues correlate with cover (supracrustal) rocks whereas the greenish and/or brownish hues reflect basement rocks (granitoid rocks and/or gneiss). The apparent boundary between the cover and basement rocks is very sharp in places and diffuse in others and differs in places from what has been mapped. Specifically, an area characterized by a magenta-purple hue (A) correlates with carbonate rocks (calc-silicate, marble). This is likely due to the calc-silicate composition in the rocks giving relatively higher reflectance values in band 5, and the carbonate composition giving relatively low reflectance values in band 7. Compositional layering (60–300 m) is clearly seen within the basement rocks (B) and within the cover rocks, especially in the nose of a plunging anticline (C). Although these hue variations have not been checked in the field, it is apparent that the Landsat data is offering information not contained on the regional geology maps. A broad zone of bluish hues (D) may represent an area of ultramafic rocks that are appear more extensive than what has been mapped. The red hues (E) represent vegetation and is found proximal to river valleys within the study area.

Less lithological information is present on the Radarsat image (**Fig. 3**b) although banding may reflect lithological differences due to differential erosion. Fold patterns are clearly seen on all the imagery. Folds are identifiable on the Landsat data due to reflectance differences defined by contrasting hues that reflect compositional layering. The fold patterns are evident in the Radarsat image due to variations in radar reflectance due to topographic changes and surface morphology. The radar image used here was acquired using a relative steep incidence angle (S2 ~ 28°), which preferentially enhances topographic and/or structural patterns (as opposed to radar images acquired at more shallow incidence angles, such as S6 and S7 ~ 40°). These features are also enhanced because the look direction is orthogonal to the structural grain, which assists in enhancing structural patterns. Both the effects of radar incidence angle and look direction on topographic and/or structural enhancement are well known (Harris and Slaney, 1982; Harris, 1986; Radarsat International, 1996). The airborne magnetics image also shows plunging fold structures due to differences in magnetic susceptibilities between lithological units; however, the lower resolution (800 m grid cell) provides less detail than the Landsat image.

Figures 4 and **5** show imagery in the southeastern portion of the study area (*see* **Fig. 2** for location). Figure 4a shows the mapped geology, Figure 4b an orthophoto, Figure 4c a Landsat TM colour composite (same band combination as **Fig. 3**a), and Figure 4d a Radarsat image (S2). Figure 5 shows a detailed view of the raw hyperspectral data for the centre of this subarea. The hyperspectral data is a RGB colour composite using narrow bands centred on the approximate same wavelength position as the Landsat TM colour composite image (*see* description for Fig. 3).

The orthophoto (Fig. 4b) lacks spectral detail, as it is very broad band data comprising the entire visible portion of the electromagnetic spectrum; however, two areas, perhaps representing different lithologies, can be seen at locations A and B. Furthermore, the orthophoto provides details with respect to the structural features, mostly because of the snow patterns that fill subtle topographical lows that follow less competent lithological units and fractures and/or faults. The Landsat image (Fig. 4c) provides more detailed information with respect to compositional layering (*see* locations C, D, and E) than the radar image (Fig. 4d). The Radarsat image enhances the structural patterns due to the relatively steep incidence angle of the S2 beam mode and favourable look direction with respect to the orientation of geological layering and structures. As expected, the increase in spatial and spectral resolution in the hyperspectral data (Fig. 5), in combination with the continuity of the spectral range between the VNIR and SWIR portions of the spectrum, provide the ability to discriminate compositional layering and lithological patterns in greater detail than the other image types. A mushroom-style interference fold is especially visible on the hyperspectral due to the ability to discriminate continuous compositional layers circumscribing the fold closure. The level of detail, with respect to both structural and lithological information, can be clearly seen in the hyperspectral image. This is typified by compositional layering which is likely reflected by layers ranging from 2 m to 10 m in thickness, and relatively continuous around the fold closure. This layering likely reflects the internal compositional layering in the Lake Harbour Group rocks, which is not differentiated on the compilation map. It is important to note that this analysis was conducted on the ‘raw’ hyperspectral data. Instrumental and atmospheric calibration and corrections were not applied at the time this analysis was conducted.

SUMMARY

The results presented here are preliminary, as they have not been followed up by fieldwork to confirm the relationship between differences in hues with respect to compositional layering as reflected by different rock types and mineralogy. Fieldwork is required to collect spectral measurements and rock samples to calibrate the range of spectral signatures apparent on the hyperspectral and Landsat data; however, visual interpretation of especially the Landsat and hyperspectral data, indicates that useful information with respect to lithology and compositional layering and structure can be obtained.

Research over the next two years will concentrate on geologically calibrating the apparent differences in spectral (hue) patterns seen on both the lower resolution Landsat and higher resolution hyperspectral data with respect to lithological and/or mineralogical characteristics. This will be accomplished by comparing spectral signatures evident on the remotely sensed imagery with ground-based spectral measurements and geochemical and petrographic analysis of rock samples collected in the field. Specifically, a spectral and compositional variance analysis will be conducted along a traverse of the Narsajuaq Arc granitic rocks in the central portion of the study area (**Fig. 2**).

The field and laboratory spectral calibrations will be used as ground truth control for the advanced processing and interpretation of the hyperspectral data. This will include comparing various supervised and unsupervised classification techniques, spectral end-member mapping (by rock type and mineralogy), as well as alteration target mapping. Application of these data is expected to provide more detailed information on the spatial distribution and patterns of the various rock types and associative mineralogy, as well as meso-scale structural features. Compositional and structural relations derived from this level of detail may reveal new information on the tectonic history of the McKellar Bay area.

ACKNOWLEDGMENTS

Funding for the project has been provided by the GSC Proposal Acceptance System and through a contribution from the Qikiqtaaluuk Corporation.

REFERENCES

Clark, R.N.
1999: Spectroscopy of rocks and minerals, and principles of spectroscopy; *in* Remote Sensing for the Earth Sciences: Manual of Remote Sensing, (ed.) A.N. Rencz; (third edition), v. 3, p. 3–58.

Corrigan, D., Scott, D.J., and St-Onge, M.R.
2001: Geology of the northern margin of the Trans-Hudson Orogen (Foxe Fold Belt), central Baffin Island, Nunavut; Geological Survey of Canada, Current Research 2001-C23, 17 p.

Harris, J.R.
1986: A comparison of lineaments interpreted from remotely sensed data and airborne magnetics and their relationship to gold deposits in Nova Scotia; *in* Proceedings of the 5th Thematic Conference, Remote Sensing for Exploration Geology, Calgary, Alberta, p. 233–249.

Harris, J.R and Slaney, V.R.
1982: A comparison of Landsat and Seasat imagery for geological mapping in difficult terrain; *in* Proceedings of the International Symposium on Remote Sensing of Environment - Second Thematic Conference: Remote Sensing for Exploration Geology, Fort Worth, Texas, p. 805–814.

Harris, J.R., Murray, R., and Hirose T.
1990: IHS transform for the integration of radar imagery and other remotely sensed data; Photogrammetric Engineering and Remote Sensing, v. 56, no. 12, December, p. 1631–1641.

Harris, J.R., Rencz, A.N., Ballantyne, B., and Sheridon, C.
1998: Mapping altered rocks using Landsat TM and lithogeochemical data: Sulphurets-Brucejack Lake district, British Columbia, Canada; Journal of Photogrammetric Engineering and Remote Sensing, v. 64, no. 4, April, p. 309–322.

Radarsat International
1996: Radarsat Geology Handbook; Radarsat International, Vancouver, British Columbia, 54 p.

Rencz, A., Harris, J., Sangster D., and Budkewitsch, P.
in press: Spectral characteristics of bedrock map units using LANDSAT TM, radar and topographic data in an arctic environment: Borden Peninsula, Nunavut Territory, Canada; Canadian Journal of Remote Sensing.

Sabins, F.
1992: Remote Sensing: Principles and Interpretation; second edition, W.H. Freeman and Co., New York, New York, 449 p.

Schetselaar, E. and de Kemp, E.
2000: Image classification from Landsat TM, airborne magnetics and DEM data for mapping Paleoproterozoic bedrock units, Baffin Island, Nunavut, Canada; *in* International Association of Photogrametry and Remote Sensing XXXIII Conference - Amsterdam, July 2000.

St-Onge, M.R., Scott, D.J., and Corrigan, D.
2001: Geology, Central Baffin Island area, Nunavut; Geological Survey of Canada, Open File D3996, scale 1:100 000.

St-Onge, M.R., Scott, D.J., and Wodicka N.
1998: Geology, Hidden Bay, District of Franklin, Northwest Territories, Geological Survey of Canada, Open File 3536, scale 1:100 000

Geological Survey of Canada Project PS1006

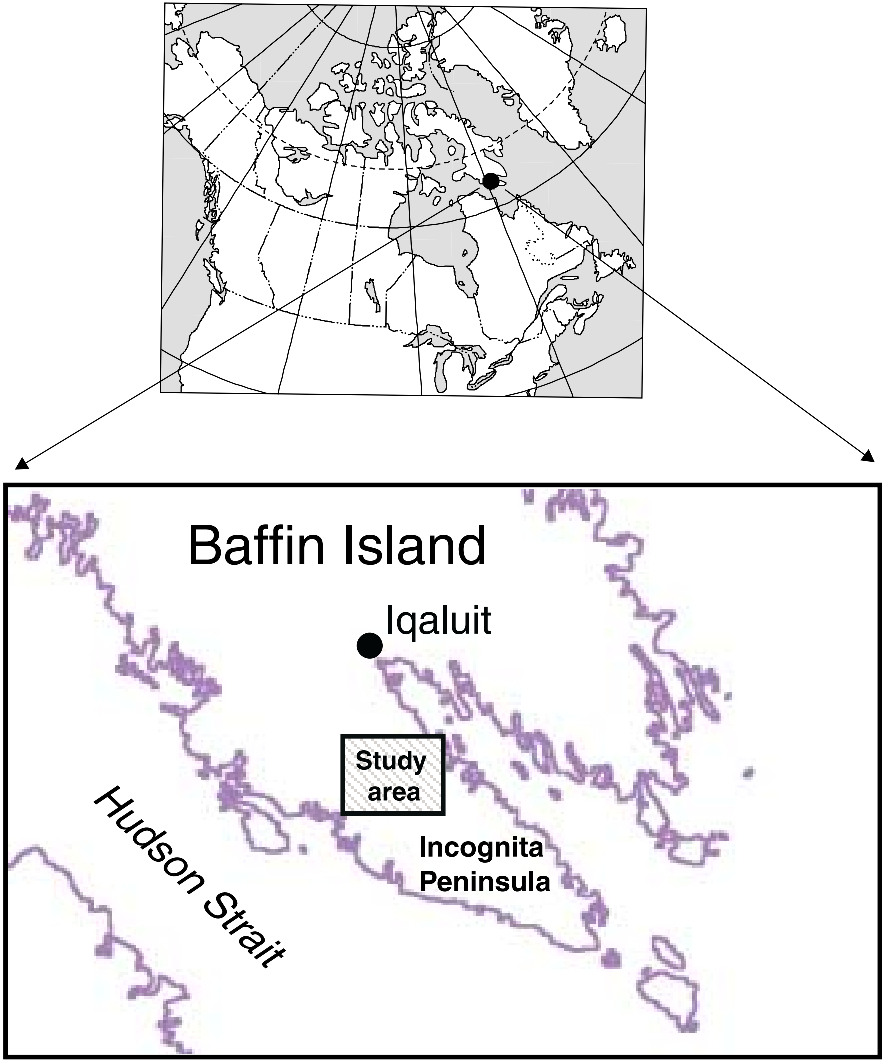

Figure 1. Location map of the McKellar Bay study area, Meta Incognita Peninsula, Baffin Island, Nunavut.

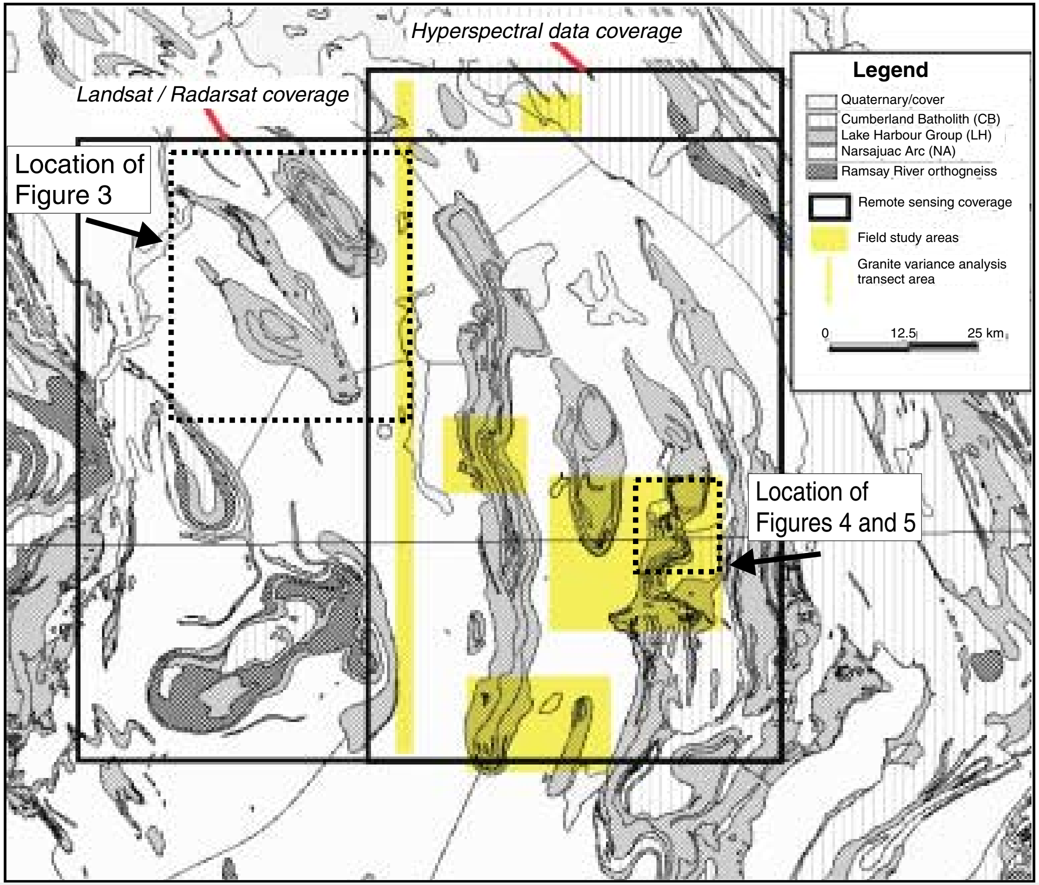

Figure 2. Generalized geology of the McKellar Bay area, Baffin Island, Nunavut. Reclassified after St-Onge (2001).

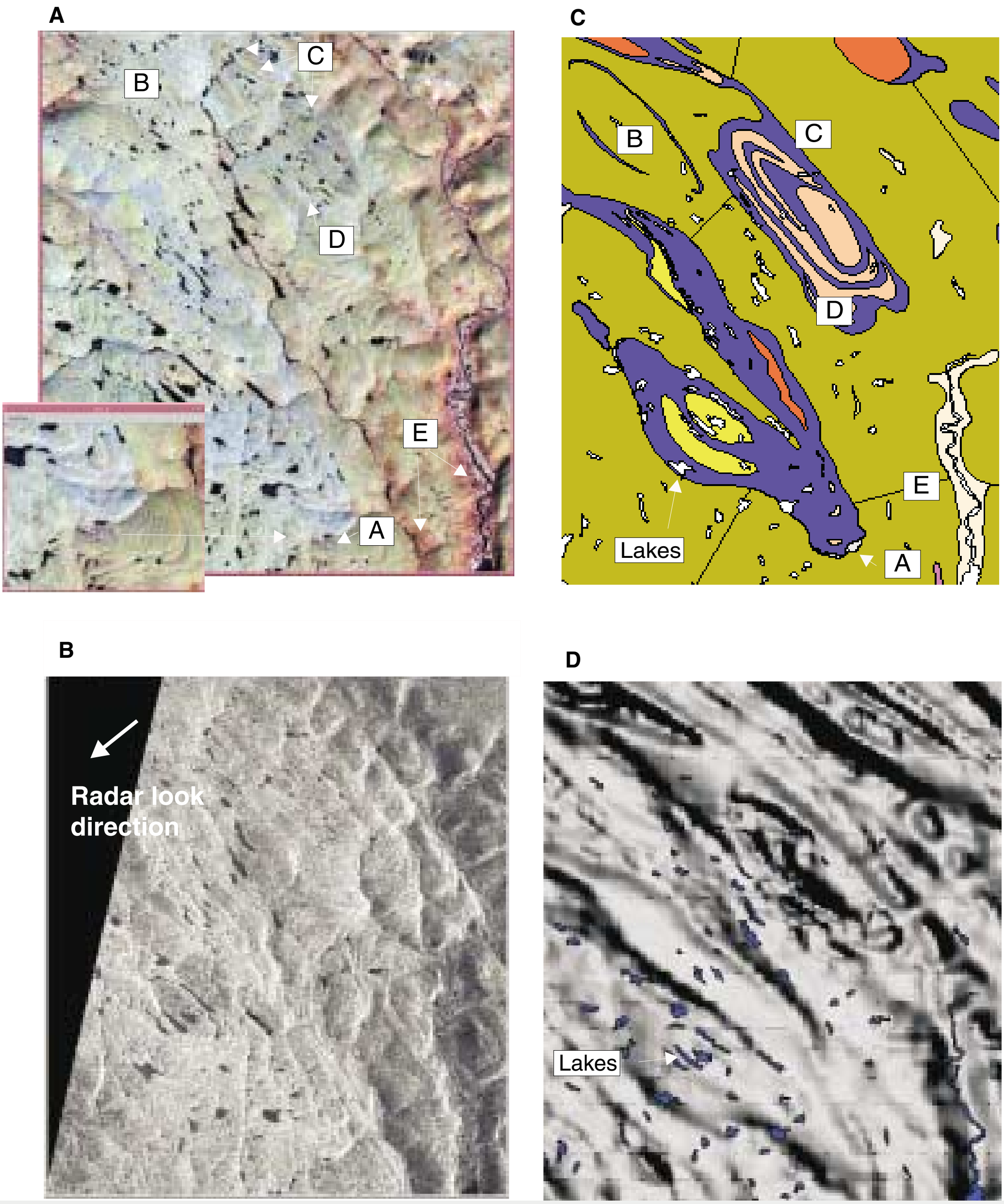

Figure 3. Comparison of **A)** Landsat, **B)** Radarsat, **C)** geological map, scale 1:100 000, **D)** shadow enhanced magnetics image. Images are not at same scale.

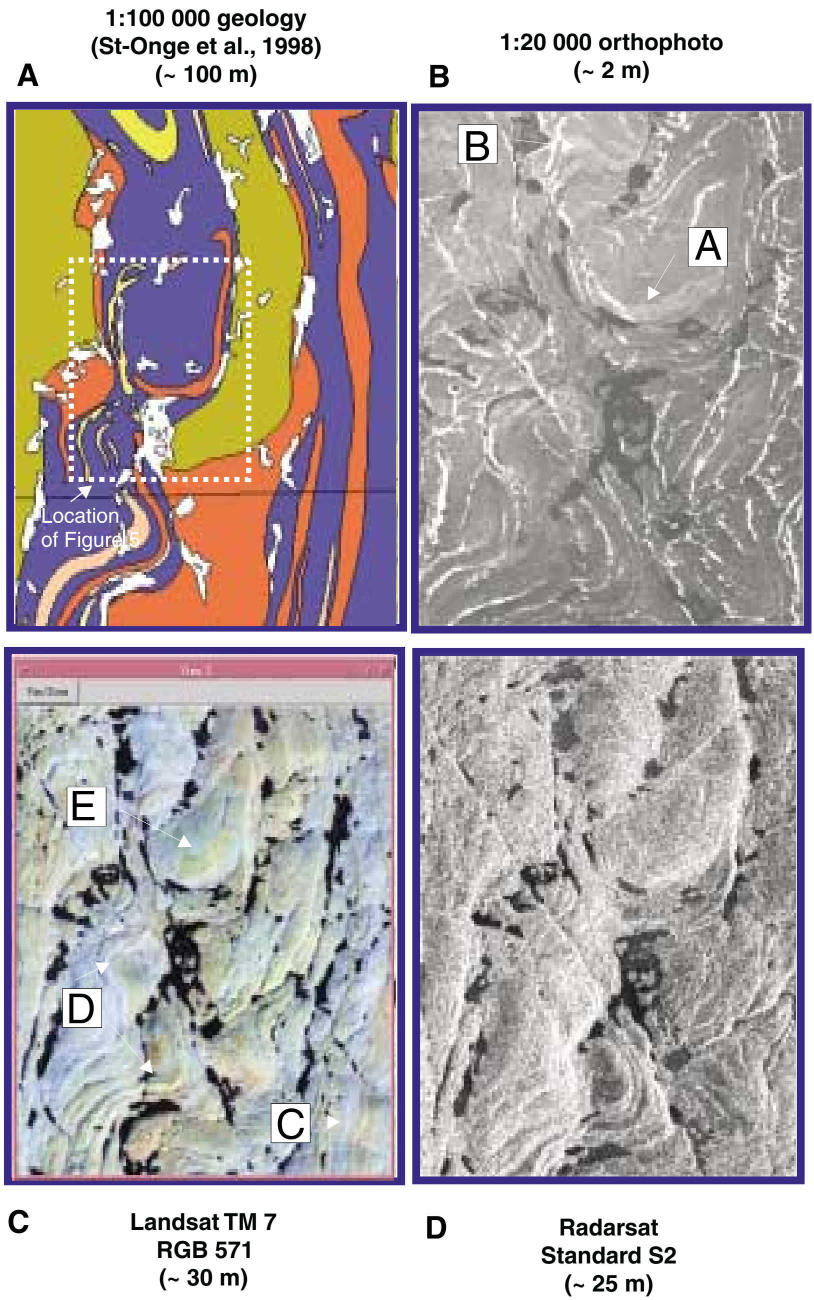

Figure 4. Comparison of **A)** geology, **B)** orthophoto, **C)** Landsat, and **D)** Radarsat data. Images are not at the same scale.

HYPERSPECTRAL
(Probe)
128 bands at ~ 5 m resolution

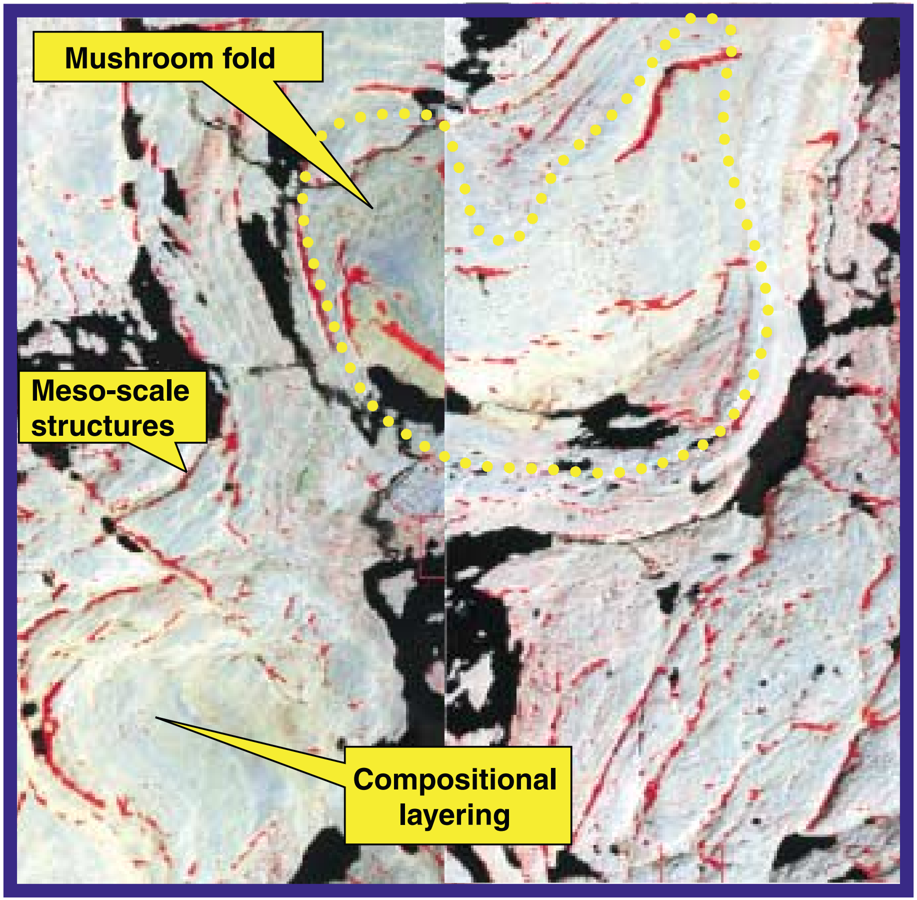

Note: 'RAW' data

See Figure 4A for location

Figure 5. View of Probe hyperspectral data for the central-east portion of the study area. Note compositional layering and the delineation of a mushroom-style fold.

Table 1. Summary of features of interest targeted for analysis from the hyperspectral and remote sensing data.

Group	Map unit and description	Features of interest
Narsajuaq Arc	Predominantly the PNm member: tonalite, granodiorite, and quartz diorite gneiss, with hornblende anorthosite layers, and monzogranite to syenogranite veins	• Compositional patterns, layering and/or variation • D_1–D_3 fabrics and relationship to compositional variation
Lake Harbour Group	PLHw: white monzogranite with metasedimentary layers PLHd: metaleucodiorite, metatonalite PLHm: metagabbro, amphibolite PLHu: metaperidotite, metapyroxenite, metadunite PLHc: marble, calc-silicate rocks PLHp: psammite, semipelite, orthoquartzite	• Compositional layering and/or variation among the different units • Relationships between structural fabric and/or orientation (D_1–D_4), and lithology and metamorphic grade/mineral assemblages (M_2) • Complex interference fold patterns are clearly revealed in some locations and can be analyzed on a meso-macro scale • Discrimination among the various igneous and meta-sedimentary rock types
Cumberland Batholith	PCmg: monzogranite, inclusions of metasedimentary rocks PCmo: monzogranite to syenogranite	• Compositional variation • Discrimination between units PCmg and PCmo • Discrimination and/or compositional analysis between Cumberland Batholith and Narsajuaq Arc on each side of northwest-southeast thrust in northeast portion of study area

Table 2. Summary and comparison of remote sensing data sources.

Data	Platform	EM spectrum range	Spatial resolution	Spectral resolution	Acquired?
Landsat 5 TM	Satellite	Optical-visible/near infrared/thermal infrared	30 m – VNIR 120 m thermal	7 broad bands (3 in visible, 3 in near infrared, 1 in thermal infrared)	Y
Landsat 7 TM	Satellite	Optical-visible/near infrared/thermal infrared	30 m – VNIR 60 m – thermal 15 m – panchromatic	7 broad bands (3 in visible, 3 in near infrared, 1 in thermal infrared)	Y
Radarsat – 2 scenes – S2 (steep - 28°), and S6 (shallow -44°) incidence angles	Satellite	Microwave	12 m	1 band (C-band ~ 6 cm)	Y
Aster	Satellite	Optical-visible/near Infrared/thermal infrared	15 m – VNIR 30 m – SWIR 90 m – thermal	VNIR – 4 bands SWIR – 6 bands TIR – 5 bands	N
Hyperspectral PROBE	Airborne	Optical-visible/near infrared	5 m	128 bands (continuous VNIR-SWIR)	Y
Orthophoto	Airborne	Visible (photo)	2 m	Visible	Y
Magnetics	Airborne	Magnetic susceptibility	800 m	1 band	Y